ABSTRACT

GOLE, NEERAJ NITIN. Transcranial Ultrasound Beam Focusing using Fast Marching Method. (Under the direction of Dr. Yun Jing.)

Transcranial High Intensity Focused Ultrasound (HIFU) has very promising therapeutic applications in treatment of brain tumor, stroke and drug delivery. Skull presents a barrier to precise focusing of acoustic waves due to refraction and scattering. To ensure focusing, phase correction is applied using ultrasound transducer array. This thesis proposes use of Fast Marching Method (FMM) to obtain the correction information. Similar to past approaches, a point source at focal point is numerically simulated. Acoustic rays are propagated through 3D skulls, using acoustic properties obtained from computer tomography of skull under study. The data containing necessary information is received outside the skull at exact locations of transducer elements. In previous researches, full wave equation was solved using conventional FDTD, k-space method etc. and hence the computation time was high. The current study will use FMM to solve the Eikonal equation. This equation makes use of bent ray approximation of waves thus reducing wave equations into a differential equation independent of frequency. The main advantage lies in the fact that while accuracy of full wave equation methods greatly depend on number of grid points per wavelength and hence resolution, FMM is far less sensitive to it. Thus one can use lower resolution for computation which greatly decreases computation time. Numerical simulations demonstrate the precise focusing with significantly lower required time, enabling pre-treatment computation on the order of seconds. The thesis also makes an important comparison between the case with and without averaging of arrival times over a transducer element. In reality a transducer element has finite dimension rather than being a single point. Thus, though the arrival times will differ across its surface,

it will emit waves simultaneously. This can add up to the error in precise focusing. The comparison reveals that the error is not very large and hence validates use of average arrival times across the surface of transducer element.

Transcranial Ultrasound Beam Focusing using Fast Marching Method

by
Neeraj Nitin Gole

A thesis submitted to the Graduate Faculty of
North Carolina State University
in partial fulfillment of the
requirements for the Degree of
Master of Science

Mechanical Engineering

Raleigh, North Carolina

2013

APPROVED BY:

Dr. Fuh-Gwo Yuan	Dr. Xiaoning Jiang

Dr. Yun Jing
Chair of Advisory Committee

DEDICATION

This thesis is dedicated

to the loving memory of my Grandmother, my biggest inspiration and a feisty lady of steel;

to all those battling brain tumor every day, you are true heroes and I hope my work helps.

BIOGRAPHY

Neeraj Nitin Gole was born on November 30, 1987 in Pune, India. He completed his primary and secondary schooling from P.E.S. NCL School, Pune and Abasaheb Garware Junior College, Pune, respectively. He then pursued his undergraduate studies in Mechanical Engineering from University of Pune, India. Working towards his Bachelor of Engineering degree, he took part in various robotic and automotive competitions. After graduation he had the opportunity to work for Mahindra and Mahindra (FES), a premier Indian tractor company. It was the passion to study further in mechanical field that led him to engage in Master of Science (Mechanical Engineering) program at North Carolina State University,Raleigh,USA. He soon developed interest in the field of acoustics, choosing it as his research area under the able guidance of Dr. Yun Jing. He worked at the Acoustics and Ultrasound Lab at NC State University from May 2012 to August 2013.

Outside of work and school, Neeraj enjoys weight training, playing tennis and trekking. He likes to spend his vacations traveling with his friends. He loves learning new sports and activities and has made most of the college recreational facilities.

ACKNOWLEDGEMENTS

I would like to thank my advisor Dr. Yun Jing for his guidance and support. His help proved instrumental in the successful completion of this thesis. I would also like to thank Dr. Xiaoning Jiang and Dr. Fuh-Gwo Yuan for accepting to be on my advisory committee.

During the one year that this research undertook to complete, there are a large number of people whose contributions were invaluable to the research. I thank my lab mates Tianren Wang and Chen Shen. Tianren's help in MATLAB coding was elemental in its optimization. I am grateful towards Dr. Jay Tu, who recommended me as grader for his course. This helped my enrollment in the Graduate Student Support Plan, which reduced the financial burden immensely. I would like to thank Sagar Vakil for introducing me to this research opportunity. A special mention to Somrita and Namita. Their help in LaTeXand composition of this thesis was invaluable.

Without the assistance and support of above mentioned people, the thesis would not have taken the current shape. I would also like to thank all my friends; Amita, Payel, Rahul, and Varun for all the weekend outings and vacations. They made these two years at school one of the most memorable experiences.

A special thanks to Girija for her encouragement and belief in me, as also improving my language skills. I am deeply thankful to my parents for their love, affection and understanding nature.

TABLE OF CONTENTS

LIST OF FIGURES

Chapter 1

Introduction

1.1 Therapeutic Ultrasound and HIFU

Ultrasound has found many applications in medical science during recent decades; from cleaning teeth in dental hygiene to treatment of cancer [5]. It has been used to relieve pain and related musculoskeletal disorders by physiotherapists[49][12]. Short ultrasound pulses can also heal fractures[6]. One such application is **High Intensity Focused Ultrasound (HIFU)**. HIFU is a hyperthermia therapy which makes use of heat to treat diseases and destroy tumors. To generate this heat locally, ultrasound energy is focused at the application point. This necessitates a precise focusing of acoustic waves to achieve maximum heat generation with minimal co-lateral damage to healthy tissue.

In 1935, Gruetzmacher discovered the physical phenomenon that using a curved piezoelectric device, short ultrasound waves can be made to focus at a point. The energy thus concentrated at the focal point was 150 times compared to the energy recorded near the same point using a vibrating plate. Pioneering work in biological application of this phenomenon was done by John. G Lynn, et al. [34]. This group also used curved piezoelectric

device. When an AC current was passed through it, the expansion and contraction of the quartz piezo crystal generated sound waves of same frequency as the current. They were thus able to produce high frequency waves. Due to the curved nature of the device, the ultrasound was focused inside fresh tissue blocks and into tissues and organs of living animals. They were able to show a local ablation at focal point while the intervening tissue remained healthy. Fry et al., in the 1950s, produced lesions and deep cuts in brains and spinal cord of cats and monkeys[21] [20]. Instead of a single focused beam of ultrasound, they used four transducers to produce as many beams to focus at a point. This helped in reduction of amount of intervening tissue, an important consideration in thin tissues like spinal cord. Though it was subsequently used for treatment of patients with Parkinson's disease and other neurological conditions [19], limitations of technology at that time restricted the progress. Several studies were conducted on viability of high intensity ultrasound in treatment of cancer[43], and its effects on various tissues was documented [3] [15] [33]. Most of the HIFU applications are still in research stages. A lot of study has been undertaken to check the feasibility of HIFU for treatment of uterine benign tumors[44], prostate cancer[39], Parkinson's disease and other neurological disorders[19].

1.2 Principle of HIFU

When acoustic wave propagates through tissues, part of it is absorbed and converted into heat. This wave can be made to focus at a point deep inside the tissue, raising the local temperature. The focus obtained is usually on the order of millimeters. By shifting the focal point minutely, or in other words focusing at different points, specific volume of tissue can be heated. The heat causes inhibition of cellular reproduction or complete destruction of tissue through ablation. In certain medical procedures like hyperthermia

or thermotherapy the temperature is maintained at around 43^0C for 60 min or longer[32]. This restricts cellular reproduction. But as treatment time is high, it is inconvenient and also allows dissipation of heat to surrounding regions thus raising the possibility of lateral damage to the tissue. On the other hand, in HIFU a very high intensity ultrasound wave is made to focus. The temperature raises rapidly up to 80^0C [45], which even for exposure of $1 second$ can cause cell death due to thermal toxicity [26]. Thus the tumor or malignant cells can be killed without damage to healthy tissue. Chen and et al. have demonstrated that exposure times of 3 s or less can effectively inhibit the chances of local thermal diffusion and heat dissipation from target region [7], thus proving the advantage of HIFU over other forms of thermotherapies. Focusing can be done by following ways:

1. Geometrically, by means of a polystyrene lens or a curved transducer

2. Electronically, by correction of phases of elements in a transducers array (phased array).

Advantages of using phased array are that the phase adjustment can be done dynamically to focus at different locations and that phase aberrations due to tissue structure can be easily corrected. To find the focal point and to guide the sound waves two methods are used:

1. Magnetic resonance imaging: This uses an MRI to locate the target volume and hence determine the focal distance. Advantage of this method, also known as MRgHIFU, lies in the fact that as MRI technology is well developed, it can be readily used for the said purpose. The disadvantage lies in the fact that separate instruments are required for MRI and HIFU due to difference in operating principles.

2. Diagnostic sonography: In this technique, acoustic waves itself are used to locate the target surface and determine the focal distance. As sonography and HIFU, both use acoustic waves, there is viability to combine them into one machine which first diagnoses for target and then treats using HIFU.

Figure 1.1 is the schematic of HIFU principle.

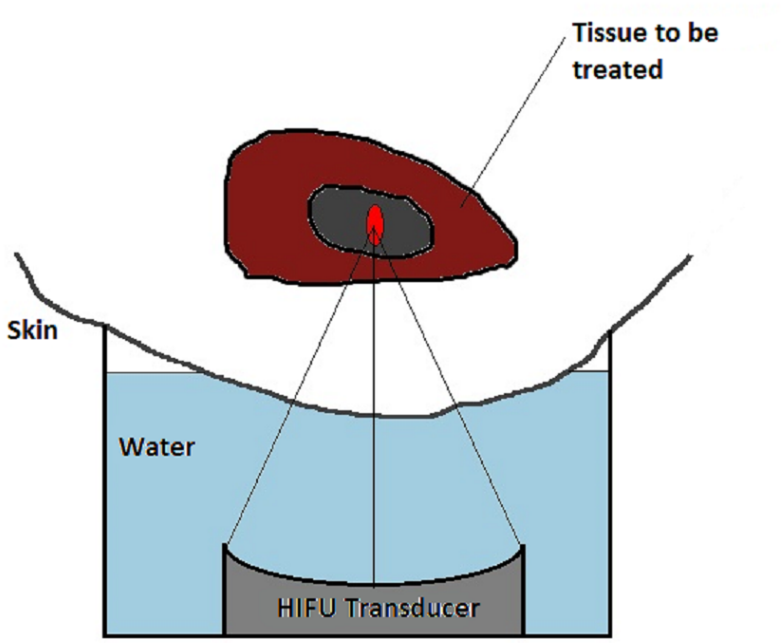

Figure 1.1: HIFU principle

The total power deposition is the amount of heat generated at a given point. It is directly proportional to absorption coefficient and summation of squared pressure, while it is inversely proportional to density and speed of sound in the medium[50]. A continuous wave excitation can have n patterns. Thus relationship for heat deposition at spatial coordinate r is given by:

$$Q(r) = \frac{\alpha}{\rho c} \sum_{n=1}^{N} p(r,n)p^*(r,n)$$

where α is absorption coefficient, ρ and c are density and speed of sound in medium respectively, and $p^*(r,n)$ is the conjugate transpose of pressure at r for nth pattern[50]. Absorption coefficient is a material property and its units are cm^{-1} and it increases with frequency. Absorption coefficient of mammalian brain at $700KHz$ is about 0.014 $neper/cm$ while it is about $0.024 neper/cm$ at $1MHz$[24]. Another important parameter is attenuation. Though absorption and attenuation are generally used interchangeably, for a narrow beam of wave, there is a fundamental difference. Attenuation includes absorption and all other losses like scattering, etc. Attenuation coefficient is always greater than absorption coefficient but varies similarly.

1.3 Advantages

1. As stated earlier, the biggest advantage of HIFU is that the tissue/ bone between transducer and target remains functioning and intact. Thus there is hardly any need for post-therapy recovery as is the case in surgical procedures. There are much lower side-effects compared to surgery.

2. Radiotherapy, chemotherapy and surgery affect the anticancer immunity of the patient leading to further complications. Ultrasound has no such effects.

3. Radiotherapy is invasive and hence needs to be given in multiple dosages, requiring the patient to attend multiple sessions. HIFU is mainly administered in a single dose thus making it more convenient.

4. Chemotherapy and radiotherapy depend on type of host tissue. Some tissues are more resilient and hence require stronger dosage to treat cancer and other malignant growths. HIFU, on the other hand, is a thermotherapy and all cells types get killed due to heat. Thus there will not be any *tumor resistance* to the treatment. Hence it can be said to be independent of tissue type to be treated.

1.4 Limitations

1. The biggest limitation is that ultrasound cannot pass through air cavity. Thus tissues inside organs with air-filled passages cannot be treated. Examples of such tumors are those inside lungs and bowel.

2. The current HIFU procedures are slow for large tumors. Thus, while is takes about $1hour$ to destroy breast tumor of $1cm$ in diameter, a $10cm$ diameter liver tumor can take more than $6hours$ for complete ablation. [31]

1.5 Time Reversal Transcranial HIFU

As mentioned in previous sections, HIFU can be used to treat tumors deep inside the tissue by ablation. This technique appears attractive in case of neuro-surgery. In many cases of brain tumor, the diseased tissue is located deep inside. Due to critical nature of brain, the conventional surgery has always been difficult and involves great risks. As HIFU techniques are non-invasive, they can be used for treating such cases without the conventional risks. As stated earlier, it was Fry et. al who first studied the effects of ultrasound focusing inside tissue of central nervous system[21] [20]. This study involved producing lesions by ultrasound focusing. Another study by Fry and Meyers in 1962 was

based on temporary modification of brain structure rather than complete ablation[17][23]. They were also able to alter the thermal dosage and maintain tissue at a particular temperature. The result was that vascular system in both grey and white matter of brain remained intact and functioning and only neural components were destroyed[22]. It was also possible to destroy grey matter (nerve cell bodies) while keeping the white matter (nerve fibres) intact. Thus HIFU can be used not only for destruction of brain tumor but also for disease like Parkinson's disease[23]. Many neural disorders involve only a small region of brain and flexibility of treating only this region while keeping rest of the tissue and its vascular system intact is a great advantage.

One of the features of transcranial HIFU which differentiates it from other HIFU therapies is that unlike HIFU therapy for prostate cancer, breast cancer, neck tumor, etc., brain is shielded by the skull. The acoustic properties of most soft tissues are similar to that water. This is because cells of soft tissues are made up mostly of water. For example, water constitutes $76-78\%$ of mammalian brain[24]. Average speed of sound in soft tissues (like brain) is $1561 m/s$[9] which is a deviation of less than 4% from that of water (which is $1500 m/s$). Noteworthy factor is that deviation within the medium (soft tissue) is even lesser. Thus for all intents and purposes, a soft tissue can be assumed to be homogeneous. The focal point (distance of target from lens/transducer) can then be easily calculated by using geometric relationship.

The study by Fry et. al[21] involved removal of bone (small portion of skull) to allow ultrasound to pass directly into brain tissue. The advantage lies in the fact that though bone needs to be surgically removed/ reflected, the brain tissue itself is untouched and lesions deep inside the tissue were achieved. In absence of bone, the tissue can be treated as homogeneous and beam could be geometrically focused. The disadvantage lies in the fact that surgery is involved which leads to healing time post therapy. Another

research by McDannold et. al also involved removal of bone. Craniotomy was performed two weeks before ultrasound therapy to allow enough time for the surgery wound to heal. The experiment was performed on rhesus monkey[38]. Thus transcranial (transkull) ultrasound focusing appears attractive option as it involves no surgery and there is little pre and post-therapy medication required.

For bones (like skull) however, the acoustic properties differ drastically from that of soft tissue or water. The density and speed of sound inside the skull is far greater than in brain. Coupling with this is the fact that skull has a highly irregular structure and shape. All this leads to failure of the homogeneity assumption as described for soft tissues. The HIFU thus gets far more complicated. Acoustic waves, like light rays, tend to bend when passing between points with a different speed. This is called refraction and it plays a major role in determining the path followed by the wave. Thus a simple geometric calculation will lead to erroneous focal distance. For this reason time reversal technique is used.

The idea of time reversal is simple and was studied for acoustics by Mathias Fink[13]. Theoretically, the classical theorems of physics are invariant in time reversal. Consider an example of a ball being thrown down from certain height h to hit a particular target on ground. Classical physics states that the ball will trace the same path but in opposite direction if it was thrown from the target to reach the height h with speed v_0, instead of being thrown down with same initial speed v_0. In other words, motion (which is a function of time) reverses direction when $t \to -t$, but the trajectory (path) remains the same. The advantage is guarantee of hitting the target. The problem with application of this property was suitable *time mirroring* to reverse time. In reality, it is not always practicable to throw the ball up from the target to study the motion *backward*. In imaging, however, we can make a movie run backwards by changing the direction in which the

recording is played[13]. Similarly if we are able to *capture* the motion of a wave originating from a point in form of images, we can *play* the images backward to make the waves travel back to the source. This is the philosophy behind time reversal. In time reversal acoustics, a small source of sound waves is located at the target by either placing transmitting device experimentally or by simulating numerically[13]. The waves from this source propagate outward, passing through the entire intermediate medium before reaching transducer elements of a phased array. The wave field is recorded at locations of transducer elements. The time can then be reversed and waves emitted accordingly by the transducer. As the waves have undergone all the possible refractions, the waves thus emitted focus back to the target. This leads to a sharp focus of high intensity; a necessary condition for HIFU. The *reversing of time* is done by emitting acoustic waves in opposite direction but with same phase as was recorded from wave originating from the point source. This is analogous to throwing the ball down with same speed but opposite direction in the above example. Experimentally placing a transmitting device has the advantage of high accuracy, but it has following limitations:

1. It might not be feasible to place the device inside a tissues and organs like brain.

2. The transducer array has to act as sensor elements leading to more costly equipment.

This leads to numerically simulating the source as an attractive option. In this method, sound speed of skull is extracted from CT scans[1]. Wave equation is then solved for a point source simulated at the target and mathematically calculated for locations of transducers. Thus by knowing the difference in these phases at different transducers, a phased array can generate acoustic waves to reach the target simultaneously.

1.6 Research Objective

Previous research on this subject involved solving full wave equation for the simulated point source to obtain phase correction. The wave equation is solved by Finite Difference Time Domain (FDTD) approach [1], or by k-space method [28]. Solving full wave equation naturally has the advantage of accuracy as the solution accounts for reflection, refraction and dispersion of acoustic waves passing through a medium. The disadvantage lies in the fact that the process is time consuming, particularly for the (FDTD). A study by Marquet et al reported computation time of 2 h for 3D simulation through the skull [36]. Solving the wave equation is resolution sensitive and requires fine mesh to correctly capture phase information leading to strain on computing resource. This problem is partly solved in k-space approach [28], which samples two points per wavelength as prescribed by Nyquist theorem. The computation time is still high.

The present study aims at improving the computational efficiency on CT based phase correction method. Instead of solving full wave equation, Eikonal equation is solved using an efficient Fast Marching Method (FMM). The chief advantage of this method is sharp fall in computation time and decrease in sensitivity to resolution. As the phase correction requires fixing the location of target from the transducers, the computation cannot be done offline. In other words, the computation time adds up to the therapy time. In practice, the target would be a small volume than a single discrete point. Thus multiple simulations will be required for set of closely spaced points. Thus it becomes crucial to have an efficient algorithm to make transcranial HIFU a viable technology.

1.7 Structure of Thesis

The second chapter deals with detail explanation of the thesis and theory behind it. It involves discussion of Eikonal equation, justification for its use and explanation of Fast Marching Method (FMM). Included in the same chapter is the derivation of Eikonal equation for acoustic waves as well as working of FMM. The third chapter consists of explanation of setup and numerical simulations carried out to justify the hypothesis. In the latter section, results are discussed in detail with comparisons to other methods. They are in form of graphs and plots. Chapter four concludes the thesis, pioneering ideas for future work.

Chapter 2

Theory

In Chapter 1, the principle of HIFU transcranial ultrasound was introduced with its application. As mentioned earlier, the previous research was based on solving the full wave equation by different methods like Finite Difference Time Domain (FDTD), K-space method, etc. This study aims at using the Eikonal equation which is a high frequency approximative method of full wave equation. The inherent advantage of this method lies in the fact that it reduces the equation into a differential equation in only spatial variable. This reduction is due to ray approximation or the Eikonal approximation.

2.1 Derivation of Eikanol Equation in Acoustics.

The wave equation in spatially dependent sound speed (as is the case in any heterogeneous medium) is given by

$$\nabla^2 p(x,y,z,t) - \frac{1}{c^2(x,y,z)} \frac{\partial^2}{\partial t^2} p(x,y,z,t) = 0 \tag{2.1}$$

Factorizing $p(x, y, z, t)$ from Eq. 3.1, we get

$$\left(\nabla^2 - \frac{1}{c^2(x, y, z)} \frac{\partial^2}{\partial t^2}\right) p(x, y, z, t) = 0 \tag{2.2}$$

For sound traversing through such a fluid, the amplitude varies with position and surfaces of constant phases can be complicated. Assume trial solution:

$$p(x, y, z, t) = A(x, y, z, t) e^{j\omega(t - \tau(x,y,z)} \tag{2.3}$$

The quantity τ is called eikonal. Substituting the trial solution in Eq. 3.2 and collecting real and imaginary parts gives

$$\begin{aligned} -\frac{\nabla^2 A}{A} + \omega^2 \nabla\tau\nabla\tau &= \left(\frac{\omega}{c}\right)^2 \\ 2\frac{\nabla A}{A}.\nabla\tau + \nabla^2\tau &= 0 \end{aligned} \tag{2.4}$$

Now from Eq. 3.4, if we have a condition that:

$$\left|\frac{\nabla^2 A}{A}\right| \ll \left(\frac{\omega}{c}\right)^2 \tag{2.5}$$

then the first equation of Eq. 3.4 assumes a much simpler form

$$(\nabla\tau)^2 = \left(\frac{1}{c}\right)^2 \tag{2.6}$$

Thus we have

$$(\nabla\tau)^2 = \left(\frac{1}{c}\right)^2$$
$$\therefore |\nabla\tau| = \left(\frac{1}{c}\right) \tag{2.7}$$

Here, $c(x, y, z)$ is function of space. By solving Eq. 2.7, we will get the curves of constant phase (wavefront) from which one can find the arrival time of this wavefront at each point in space. We can plot contours representing constant arrival time from the source. Thus we can easily find the arrival times for each of the transducer elements and phase difference across them. By correcting the phase we can focus the waves at simulated source location.

2.2 Eikonal Approximation and its Justification

Eq. 3.4 made very important assumption

$$\left|\frac{\nabla^2 A}{A}\right| \ll \left(\frac{\omega}{c}\right)^2$$

The sufficient conditions satisfying this assumption are

1. the amplitude of the wave does not change significantly over distances comparable to wavelength, i.e $\nabla A \ll \omega$

2. speed of sound does not change significantly over distances comparable to wavelength, i.e $c \ll \omega$

For a given medium, speed of sound does not change in time. The wavelength λ then varies inversely with frequency. Thus for a high frequency sound passing through a given medium, the wavelength is small. The acoustic properties of medium vary with space. This variation would be less significant over small wavelength. Hence, the usage of Eikonal equation instead of full wave equation is justified for transcranial ultrasound studies. The current study assumes linear acoustics and hence transverse dimensions are not very large. If a beam of sound wave has large transverse displacement, the assumption will fail at the edges due to manifestation of diffraction which is completely ignored in case of Eikonal approximation.

2.3 Fast Marching Method

Fast Marching Method (FMM) is a numerical method that approximates the solution to nonlinear Eikonal equation of the form

$$S(x)|\nabla g(x)| = 1 \tag{2.8}$$

FMM is a method which calculates the shortest distance from a set point/points to all other points in a grid. As sound bends *towards* the medium with higher speed during refraction, it in a way traces the path of shortest distance. Using FMM we arrive at shortest distance field. Thus we can find the difference in shortest distances from the simulated source to all the points on transducer. Necessary condition of FMM is $S(x)>0$. This means that the speed of sound is positive and the waves are monotonically advancing without reverse of direction. Comparing Eq. 2.7 and Eq. 2.8, it is realized that in this case $g(x) = \tau$ and $S(x) = c(x, y, z)$. The algorithm is similar to Djikstra's algorithm[11].

It uses upwind viscosity solution finite difference method to solve the above equation. Thus it is a special case of level set method[14]. FMM is implemented for a 3D lattice by working outwards from initial voxel (point). The steps are as follows

1. Initialization: In this step the initial voxel is set to be *current* and the distances to all its neighboring voxels are computed and put in a binary heap where the element is the pointer to each of these voxels and key is the computed distance. This binary heap forms the *unvisited* voxels in the ascending/descending order of the key value.

2. Loop: In the first step, the unvisited voxel with smallest value is set as current. Then the distance to all its neighboring *unvisited* points is calculated and tagged in the binary heap. If the neighbor was already in the unvisited heap, then the distance is simply recalculated and its position in the heap changed to reflect the new value. In the last step, the current voxel is put in *visited* set and the algorithm loops back to select the new smallest value unvisited voxel and proceeds to set it as current. Note that mere examination of distance of neighboring voxels does not make them *visited*. Only the current voxels, after the distance to their neighbors calculated and new *current* voxel set, do become *visited*

The advantage of FMM is that each voxel is visited only once and it distance is not calculated more than once. This ensures that the code runs at a great rate without repetition of the calculation [2]. This study makes use of the high accurate FMM called as *multistencil fast marching method (MSFM)*. It calculates the arrival time (which is time required to trace the shortest path from the point source) at each point in space using Eikonal equation along multiple stencils that cover its entire neighboring region and then select the one satisfying the upwind condition [25].

Figure 2.1 illustrate the idea in 2D. Figure 2.1a is the sound speed image of 2D skull with transducers in red color. Figure 2.1b is arrival time image of waves propagating through a 2D skull image. Using FMM, Eikonal's equation has been solved. Each color represents a unique *first* arrival time of the wave front. Thus we can see that the waves originate at the numerical simulated point source which is at (0,20) mm. Waves travel outward. Direction of the waves does not reverse at any instance. As the arrival time is the time required by only the first wave to reach a point is calculated, reflection and total internal refraction are not accounted. The time required for the wave to propagate to every grid point from the source is calculated. We can see that due to presence of skull, the time fronts are not symmetric and they As location of the transducer elements with respect to the grid is precisely known, one can easily find the arrival time and these elements and hence calculate the phase difference. Figure 2.2 represents arrival time images for half and quarter resolution. We can see a clear *blurring* of the image in Figure 2.2b. Figure 2.2a is sharper than the quarter resolution case but more blurred than original resolution. The sharpness of the image determines the accuracy of the arrival time data. Thus the quarter resolution is clearly not as accurate as original resolution. The results in Chapter3 will show the effect of resolution on sharpness of focus and prove the robustness of FMM to low resolution.

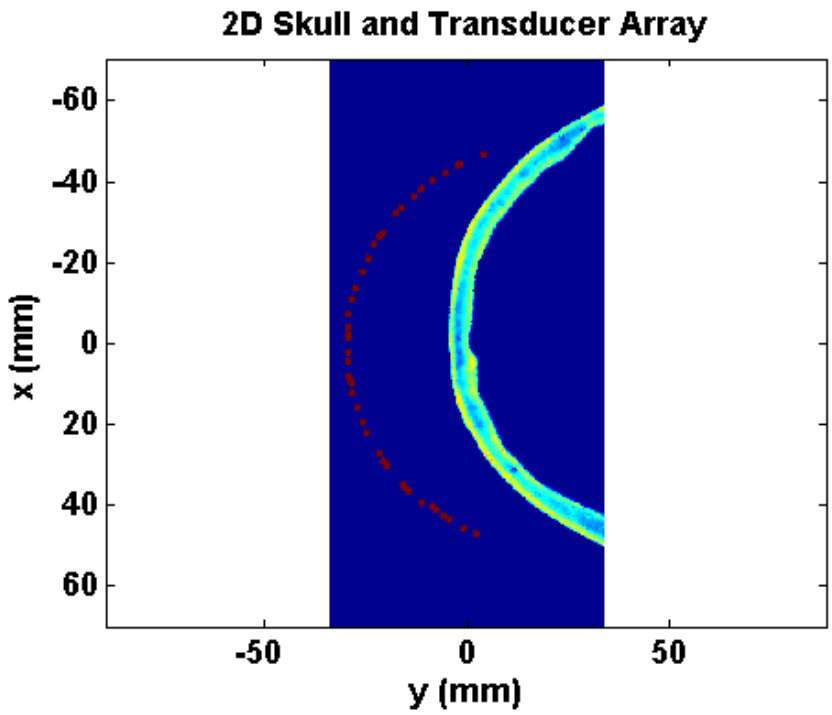

(a) 2D Skull and transducer array

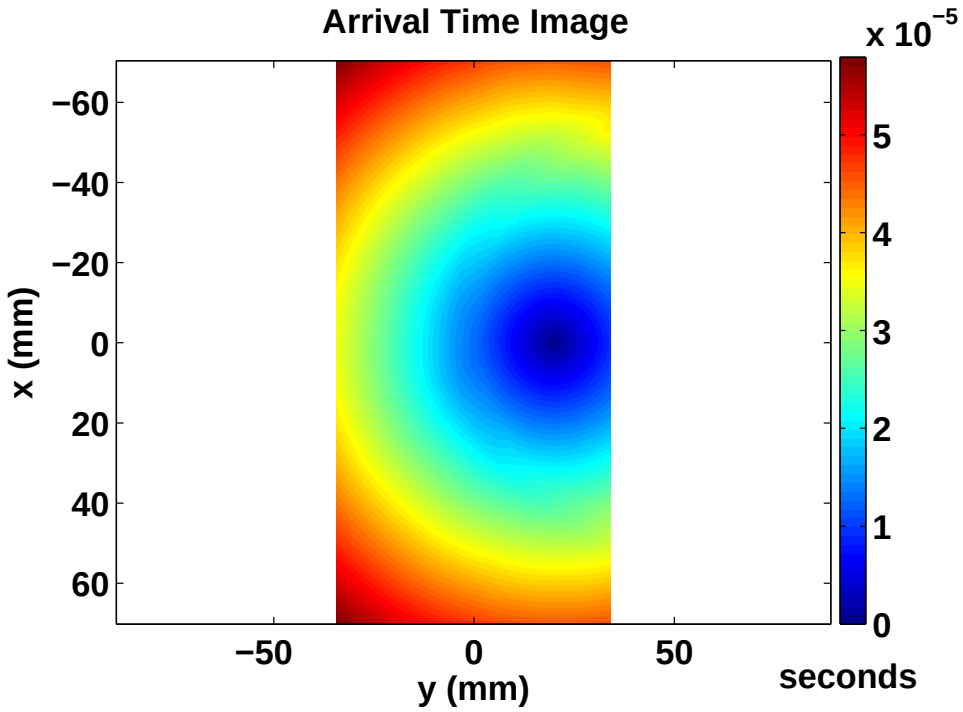

(b) Arrival time image

Figure 2.1: FMM illustration

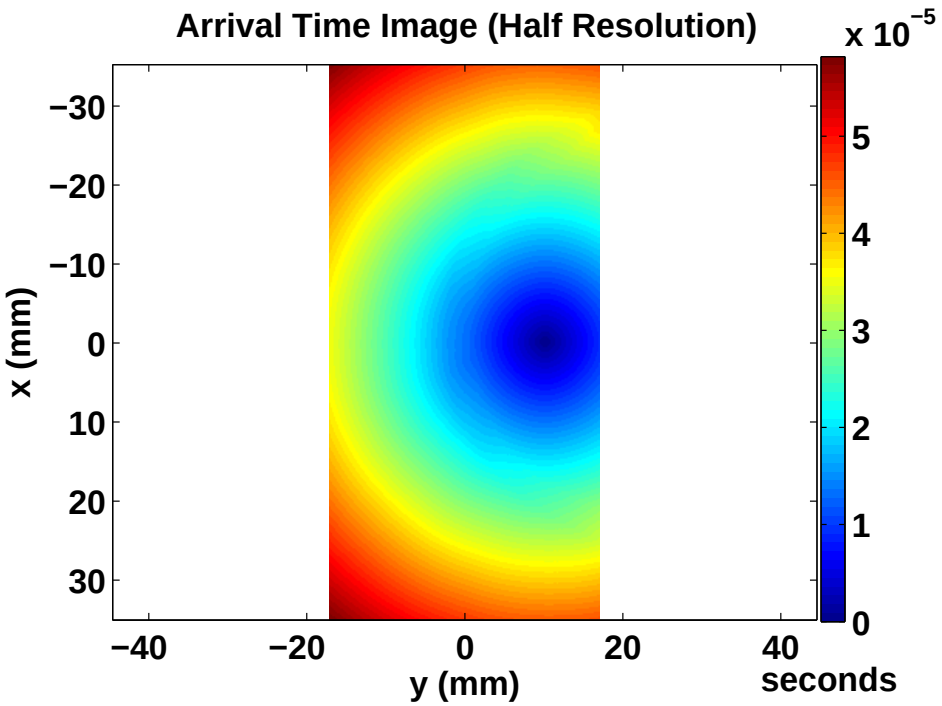

(a) Arrival time image (Half Resolution)

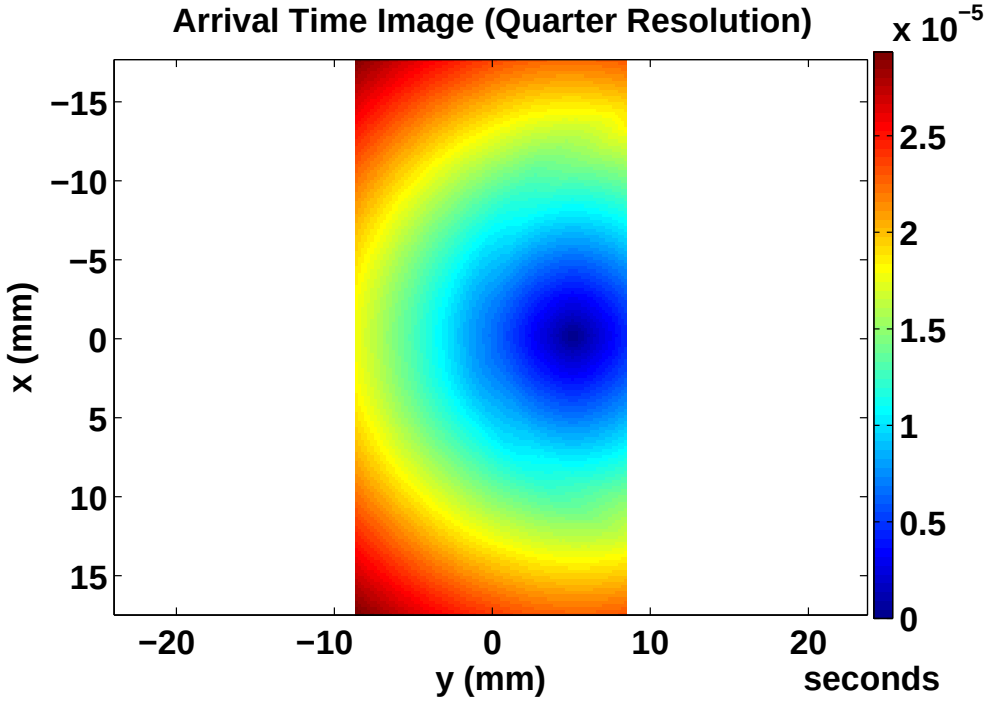

(b) Arrival time image (Half Resolution)

Figure 2.2: Arrival time image for half and quarter

2.4 Advantage of FMM over Full Wave Equation Method

The accuracy of full wave equations depends on number of grid points per wavelength, partially because of Nyquist-Shannon theorem[35]. In FMM, the wave is assumed to be a ray and close spacing of voxels is needed to accurately trace the shortest path. But it does not depend on the wavelength and hence the method is more robust to resolution. While k-space method reduces the resolution dependence compared to FDTD, it is found that FMM is far less sensitive to resolution than any full wave methods. The results of this study will prove the point. As computation time is directly proportional to resolution, use of FMM in low resolution environment can substantially decrease the required time. Also, FMM solves a differential equation in only spatial variable (Eikonal equation) instead of full wave equation which has time and space as variables. This reduces the required computation time.

2.5 Frequency Limitation

As the Eikonal approximation works the best for higher frequencies, there is a lower limit of the waves for which the simulation will hold true. Increasing the frequency leads to a sharper focus as the properties of medium change gradually with respect to the wavelength of sound in such a case. Although, for waves of even higher frequencies the approximation will hold true, the limiting factor is that high frequency waves are absorbed at higher rate by skull causing local heating. Diploe is a soft spongy bone structure found in between outer and inner layers of skull. Studies have shown that sound pressure attenuation coefficient increases from around $1\,cm^{-1}$ at $500KHz$ to little more than $2\,cm^{-1}$

for $1MHz$. For skull along with all the components, the attenuation coefficient rises from about $1.8\,cm^{-1}$ to $2\,cm^{-1}$ for frequencies from $500KHz$ to $1MHz$[18]. Thus there is a sharp increasing in attenuation coefficient for diploe. Attenuation is due to absorption and scattering. The absorbed energy is converted to heat and there is an increase in temperature of skull along the path of ultrasound beam. This can be dangerous. Hence the current study is for two frequencies: $670KHz$[37] and $1MHz$[36]. These are also the frequencies widely studied for transcranial HIFU.

Thus theoretically, solving the wave equation is more accurate than Eikonal equation. The tradeoff is between accuracy vis-à-vis computation time of FMM. In the proceeding chapter, the study compares this aspect by presenting the findings with discussions on each of them.

Chapter 3

Results and Discussion

3.1 Simulation Setup

3.1.1 Explanation of Different Cases

This chapter presents findings of the current study. As stated, the objective is to test the accuracy and required computation time of FMM and compare it with the k-space method which solves the full wave equation. The accuracy is tested by comparing the focus obtained by these two methods on the planes passing through the numerically simulated *source* point. In all the simulations, the source has been placed at the center of spherical binary mask representing the transducer (phased array). To demonstrate the necessity of phase correction, results obtained without applying any phase correction have been included. The model is a 3D binary grid. To accurately represent finite transducer surface area, several grid points together form a single transducer element. Thus the arrival time for one particular element is the average of arrival timesrecorded on each of the grid points forming the element. As this may add a small error in phase correction,

comparison was done for cases with and without taking this average was made for 1 MHz. For each case, acoustic energy (normalized pressure square distribution) was measured on the X-Y, Y-Z and X-Z planes passing through the point source (a focal point). In the forthcoming sections, this has been shown by making use of contour plots. Energy distribution along X-axis at the focal point is also captured and compared for different cases via graph plot.

3.1.2 Use of k-Wave Toolbox

For the k-space method, the wave needs to be simulated, originating from the point source. The pressure field is recorded at the locations of transducer for discrete time intervals. Fast Fourier transform is used to express the pressure field in frequency domain. The phase of the peak pressure to reach each grid point forming transducer elements is recorded. Thus the phase delay between each element can be found out and correction applied. The current study is non-experimental and hence forward propagation (waves from transducer to the focal point) needs to be simulated for both, FMM and k-space method. These wave simulations are done using an open source MATLAB toolbox called k-Wave[46]. The toolbox solves the equivalent forms of generalized Westervelt equations using k-space pseudo-spectral method. Here, the temporal gradients are solved using k-space finite difference scheme[48]. The k-Wave toolbox is able to simulate nonlinear waves through heterogeneous medium as also account for power law acoustic absorption[47]. However for the present study, nonlinearity and attenuation are not considered.

3.1.3 Model

The skull speed image is obtained from computer tomography (CT scan). Acoustical properties are derived from CT scans[1]. Density is given by

$$\rho = \phi \times \rho_{water} + (1 - \phi) \times \rho_{bone} \tag{3.1}$$

where ϕ is porosity given by

$$\phi = 1 - \frac{H}{1000}$$
$$H = 1000 \frac{\alpha_x - \alpha_{water}}{\alpha_{bone} - \alpha_{water}} \tag{3.2}$$

H is the Hounsfield units. Here α_x, α_{water} and α_{bone} are linear photoelectric attenuation coefficients for the part of tissue under consideration, water and bone respectively. If the skull is completely degassed and placed in water, porosity in the bone will be completely filled with water. The structure is thus made up of bone and water alone[1]. We can then propose a linear relationship between attenuation coefficients given by:

$$\alpha_x = \phi \times \alpha_{water} + (1 - \phi) \times \alpha_{bone} \tag{3.3}$$

In Eq. 3.1, ρ_{water} is set as $1500 kg/m^3$. ρ_{bone} is the maximum density of human skull. Using the average density found from statistical studies[18] and taking into consideration the heterogeneity of inner table of skull, ρ_{bone} is set as $2100 kg/m^3$[1]. Similarly speed of sound is given by

$$c = c_{water} + (c_{bone} - c_{water}) \times (1 - \phi) \tag{3.4}$$

Here sound speed in water which is $1500m/s$ is assumed as minimum speed in skull or tissue[1]. The c_{bone} is again found from statistical studies by Fry et. al. [18] and set as $2900m/s$.

The sound speed image for this study is only of a portion of skull. The reason for this is computational resource limitation. As the study compares FMM with k-space method, wave equation needs to be solved for the latter and it is the limiting factor. However, study using larger portion of skull can be carried out by FMM using lower resolution. More explanation on this topic is given in Chapter 4. The spatial dimensions of the model are $180 \times 180 \times 90mm$ and the spatial resolution is $0.1953mm$. Wavelength is related to frequency by

$$\lambda = \frac{c}{f}$$

where c is speed of sound in medium and f is frequency. Therefore in water, for $1MHz$ frequency, wavelength is $\lambda = \dfrac{1500m/s}{1 \times 10^6 Hz} = 1.5mm$. Thus resolution of $.1953mm$ is sufficiently smaller compared to wavelength and there are around 7 grid points per wavelength. This is of importance in k-space method. Similarly, for $670KHz$ wavelength $\lambda = 2.3mm$ and there are about 11 grid points per wavelength. The transducer phased array has geometry that a spherical cap of radius $84mm$. There are total of 93 transducer elements with each having dimension of $11.7 \times 11.7mm$. The skull speed image and transducer array are located as shown in Figure 3.1. The skull speed image is shown in blue shade while the transducer is in red. Through out the study, point source (focal point) is at the geometrical center of the *spherical* transducer array. Coordinates of point source are $(0, 0, 41)mm$. For the simulations, a numerical grid was created with monotonically increasing spatial dimensions.

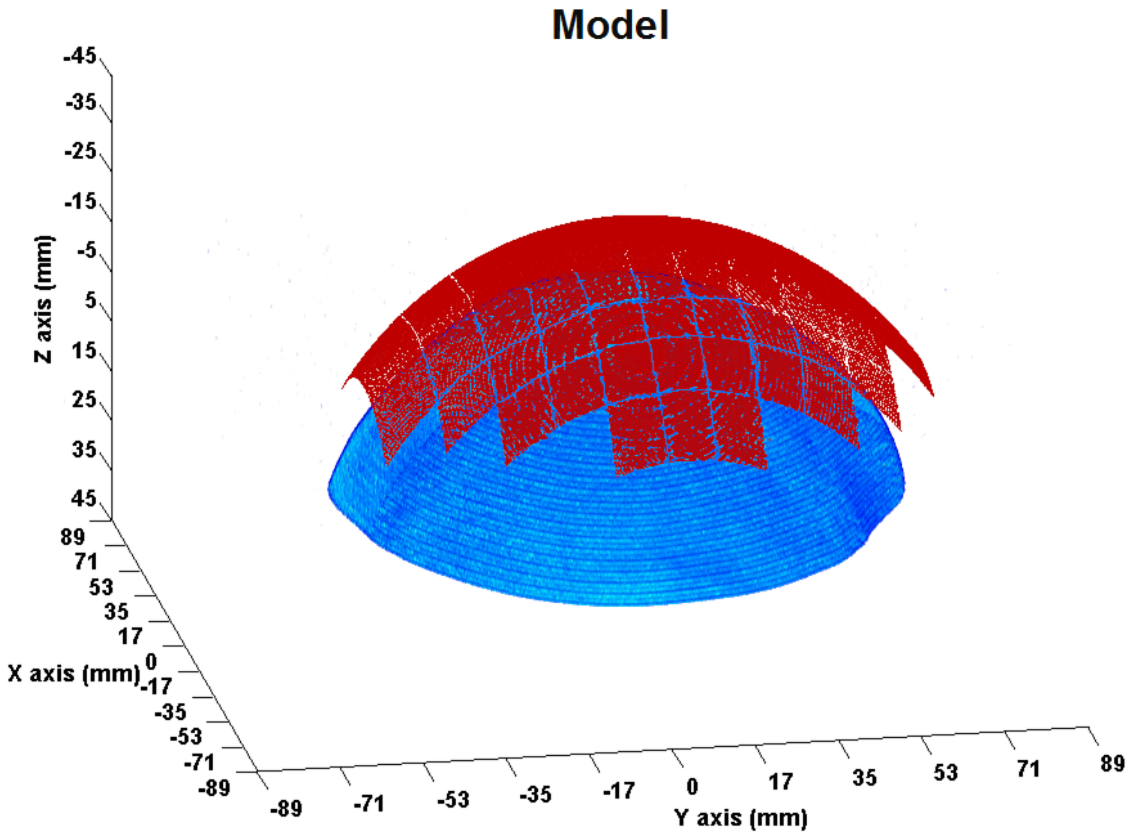

Figure 3.1: Model

3.2 Focal Plane Contour Plots

These are the contour plots of energy distribution on the XY, XZ and YZ focal planes. The results are presented in form of subsections, each one representing one case. $1MHz$ frequency was used more extensively, including all the different cases like with/without averaging for transducer elements, original and coarse resolutions, etc. Hence it is presented in the beginning sections followed by certain cases for $670KHz$. The point source (focal point) for all the cases is at $(0, 0, 43)\, mm$

3.2.1 $1MHz$ Without Phase Correction

To illustrate the need of phase correction in transcranial ultrasound propagation, a trial has been shown in which no correction was applied. As the target point is at the geometrical center of spherical transducer array, the waves were simulated to emit in phase (simultaneously) from all the elements. As can be seen from Figure 3.2, without any phase correction the focus is not sharp. There are large areas away from focal point especially in the X-Y and X-Z planes. In X-Y and Y-Z planes, these areas have energy level of 500 units which is $7 - 8\%$ of the maximum energy which is at geometrical center (location of point source). In YZ focal plane also the distribution is not precise. Thus correction is necessitated.

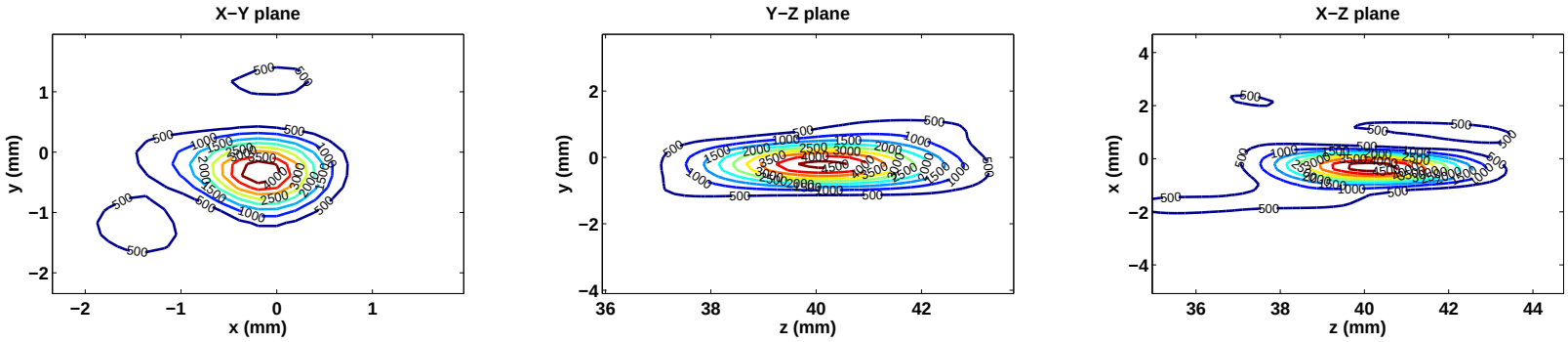

(a) (b) (c)

Figure 3.2: $1MHz$ without correction

3.2.2 $1MHz$ Fast Marching Method

This is result for phase correction applied by using FMM. Comparison with Figure 3.2 shows that the focus is much sharper in Figure 3.3. Also the energy level is far higher. While the maximum amplitude in the case without correction was about 4500, it is around 7000 in FMM. The contours at the boundaries have far less levels in this case. Also, the energy quickly falls from focus to outer contours in space of $3mm$. Thus there is minimal energy concentration in healthy tissue while giving highest energy at the point source. **The computation time was around 23 *minutes***

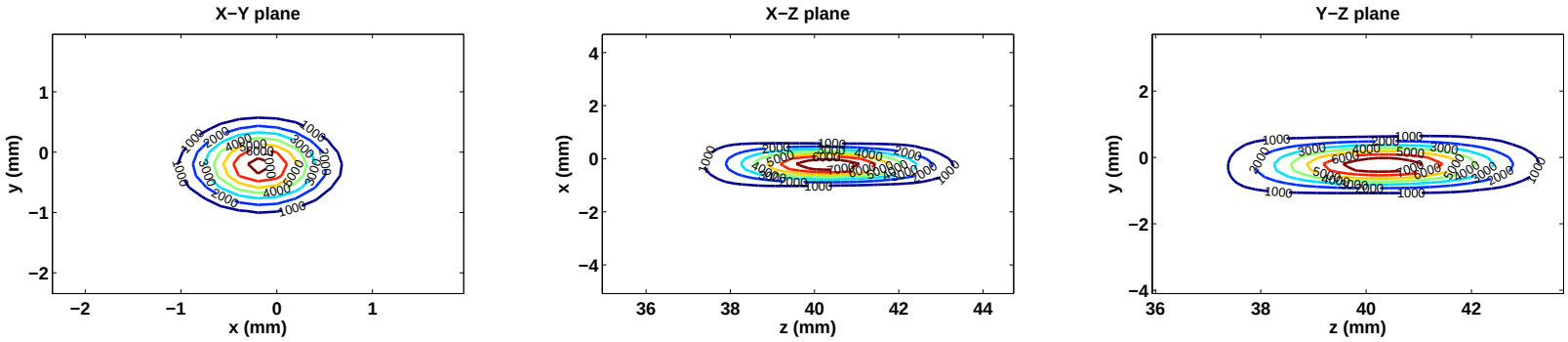

(a) (b) (c)

Figure 3.3: $1MHz$ fast marching method

3.2.3 $1MHz$ K-space Method

The k-space method also gives a sharp focus. There is very less to distinguish between the acoustic energy contour plots for fmm and k-space method (Figure 3.3 and Figure 3.4). Again, the energy levels are high with inner contours at 6000, while it falls quickly to 1000 units. The significant parameter is **computation time**. k-Wave took about $\mathbf{24}\boldsymbol{hours}$ for the simulation with the same numerical grid size, speed image and transducer mask as was in the case of fmm.

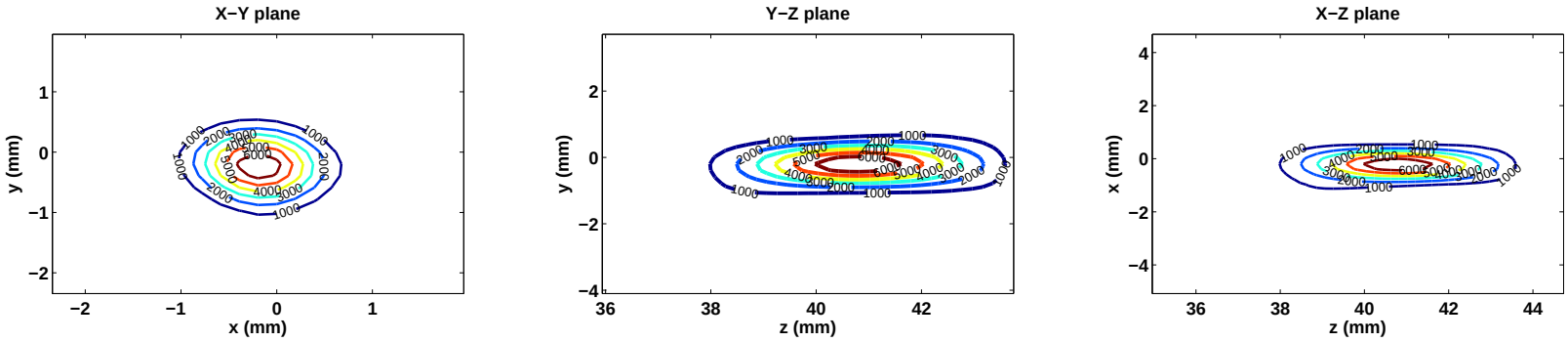

(a) (b) (c)

Figure 3.4: $1MHz$ k-space method

3.2.4 $1MHz$ Fast Marching Method Without Averaging

As mentioned earlier, a number of grid points form a single transducer element. In this study 3600 grid points were used to define each element which has size of $11.7 \times 11.7mm$. In reality the element will emit waves in a single phase, thus average of arrival times at all the grid points of an element is taken. This can account for some error and hence this case is presented wherein each grid point has its own recorded phase and no average is taken. As expected, the results are more accurate as compared to the FMM with averaging case. Figure 3.3 shows a maximum of 7000 while Figure 3.5 has 9000 units. But the focus is not significantly sharper. The difference in amplitudes is also tolerable. **Computation time: 22 *minutes***

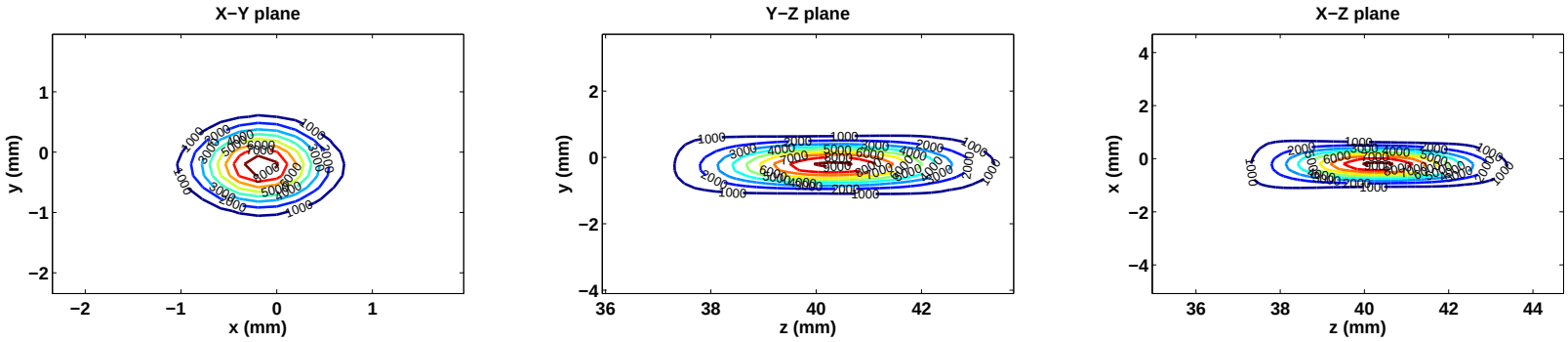

(a) (b) (c)

Figure 3.5: $1MHz$ fast marching method (without averaging)

3.2.5 $1MHz$ K-space Method Without Averaging

This case is similar to previous one but using k-space method. Compared to the one with averaging (Figure 3.4), the focus is slightly sharper and has higher amplitude. With regards to Fast Marching Method, without averaging, again k-space method gives better results than FMM; but the difference is not significantly large. These two cases validate the averaging over the grid points forming transducer element. The maximum energy is at focus and equal to 9000 units (in Y-Z plane) while it falls to 1000 units over maximum distance of around $3mm$. **Computation time: 24*hours***

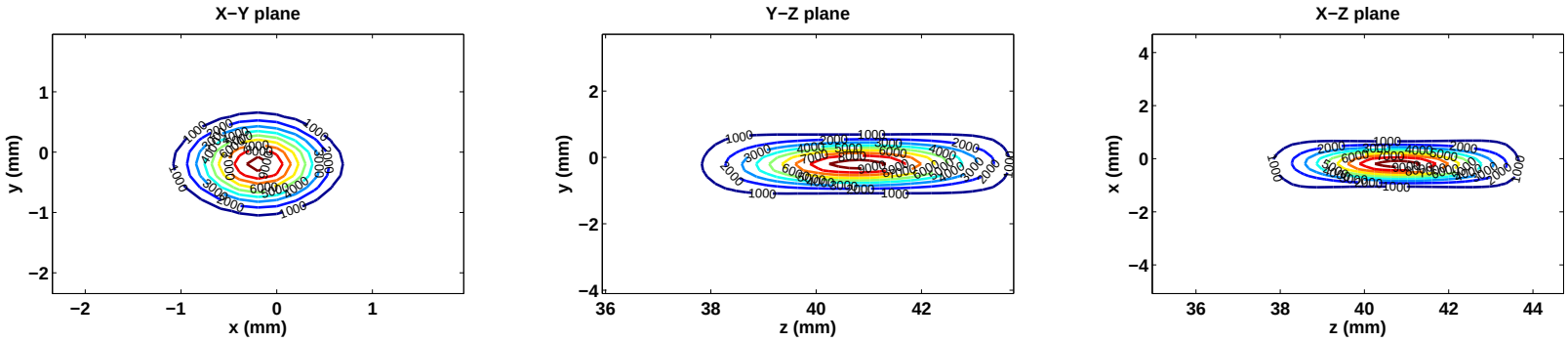

(a) (b) (c)

Figure 3.6: $1MHz$ k-space method (without averaging)

3.2.6 $1MHz$ Fast Marching Method With Half Resolution

Full wave equation methods have susceptibility to resolution. The accuracy diminishes with lowering of resolution. The FMM, theoretically is insensitive to resolution. Numerical calculations demand sufficiently close grid spacing. to test the robustness of the method to spatial resolution, cases were studied for half and quarter of the original resolution. This is the case for one half resolution with spatial resolution dx= 0.39706. Thus the wavelength of sound through water at $1MHz$ ($\lambda_{1MHz} = 1.5mm$) is 4 times the grid spacing. There is very little to differentiate between half and original resolution cases. However, the computation time decreases by an order of over 12.4 **Computation time: 1.86 *minutes***

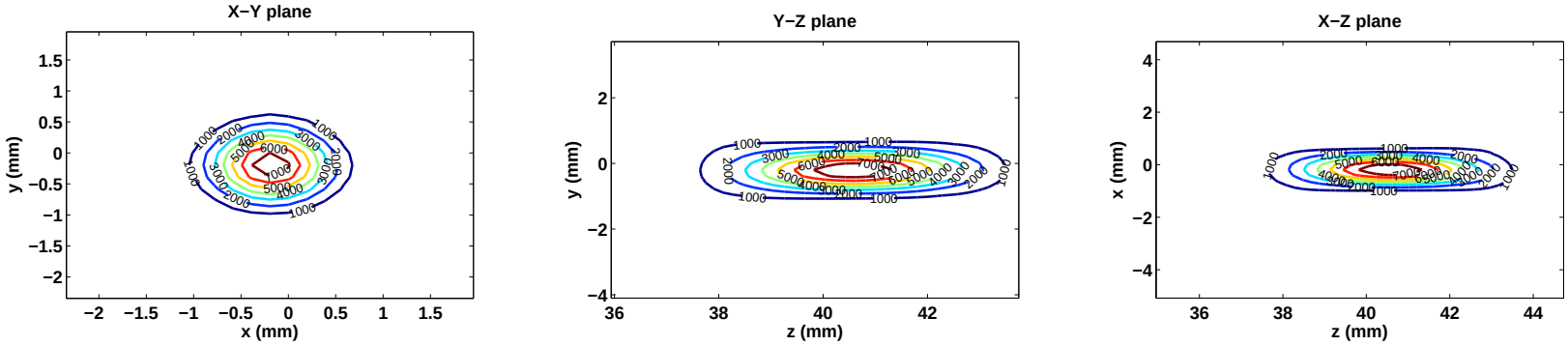

(a) (b) (c)

Figure 3.7: $1MHz$ fast marching method with half resolution

3.2.7 $1MHz$ Fast Marching Method With Quarter Resolution

For quarter resolution case, spatial resolution dx=.7812 which is around half the wavelength of sound through water at $1MHz$. Thus, there are around 2 grid points per wavelength which is the lower threshold for k-space method. This case has slightly lesser amplitude at the focal point as will be presented in the X *axis* plots. But the focus is equally sharp. Thus these trials prove the high immunity of FMM to resolution variation. Computation time decreased sharply. Thus there is a possibility of use of low resolution speed images in case of FMM unlike for full wave methods. **Computation time: 8.4 *seconds***

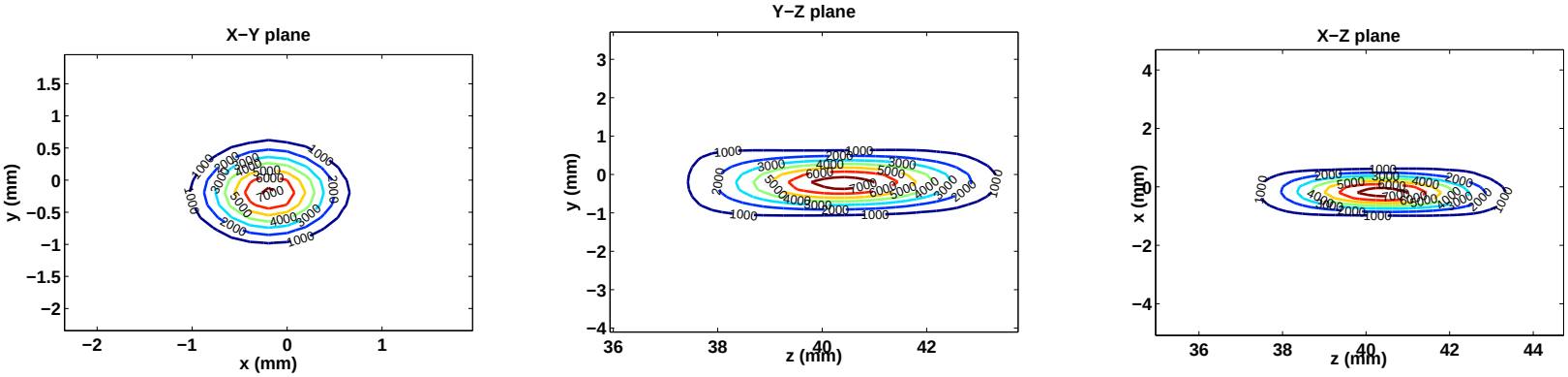

(a) (b) (c)

Figure 3.8: $1MHz$ fast marching method with quarter resolution

3.2.8 $670KHz$ Without Phase Correction

From here on, results for $670KHz$ frequency are presented. As is in the $1MHz$ case, phase correction is necessary. Without correction the focus is not sharp and there are energy peaks away from the point source, thus being potentially harmful. Figure 3.9 proves this point. In the X-Y plane, there is a high energy region centered at around (-1.8, -2). This is a secondary focus with energy of 500 units. Compared to the primary focus of 5000 units at (0, 0), it is almost 10%. Such a high energy secondary focus is very harmful to healthy tissue. X-Z and Y-Z planes also show dispersed focus.

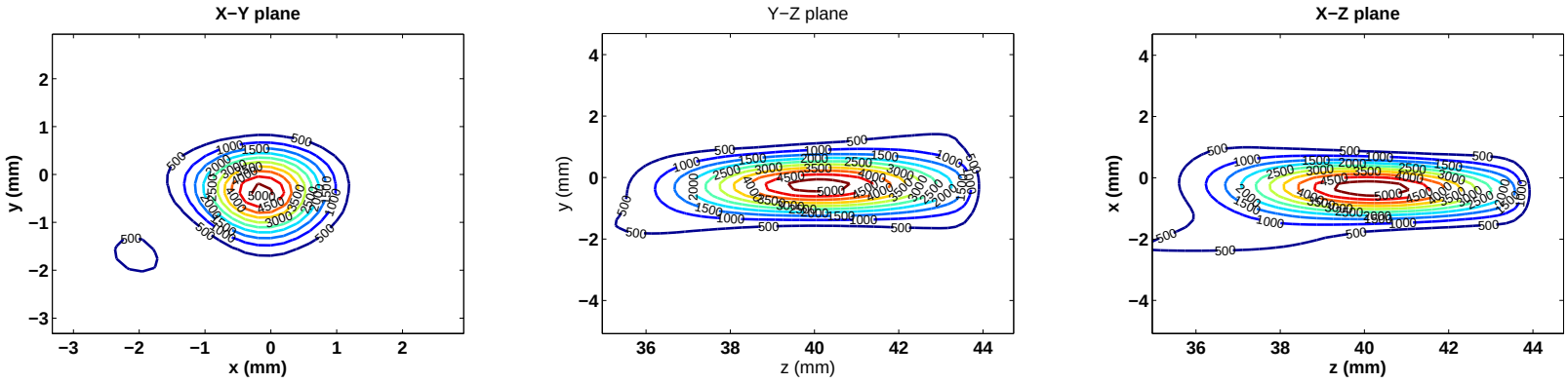

(a) (b) (c)

Figure 3.9: $670KHz$ without correction

3.2.9 $670KHz$ Fast Marching Method

Again, the focus is sharp with maximum energy of 600 units which decreases to 1000 in maximum space of $4mm$. Comparing the following figures with Figure 3.3 (1MHz case), we realize that in YZ and XZ focal planes, the maximum amplitude is slightly lower in $670KHz$ case. It has reduced from 7000 to 6000 units. Focus is also slightly less sharp. This could be because of the theory that Eikonal equation is a high frequency assumption and hence $1MHz$ has better results as compared to $670KHz$. The difference, however is not very large and hence Eikonal's approximation still holds true. **Computation time: 21 *minutes***

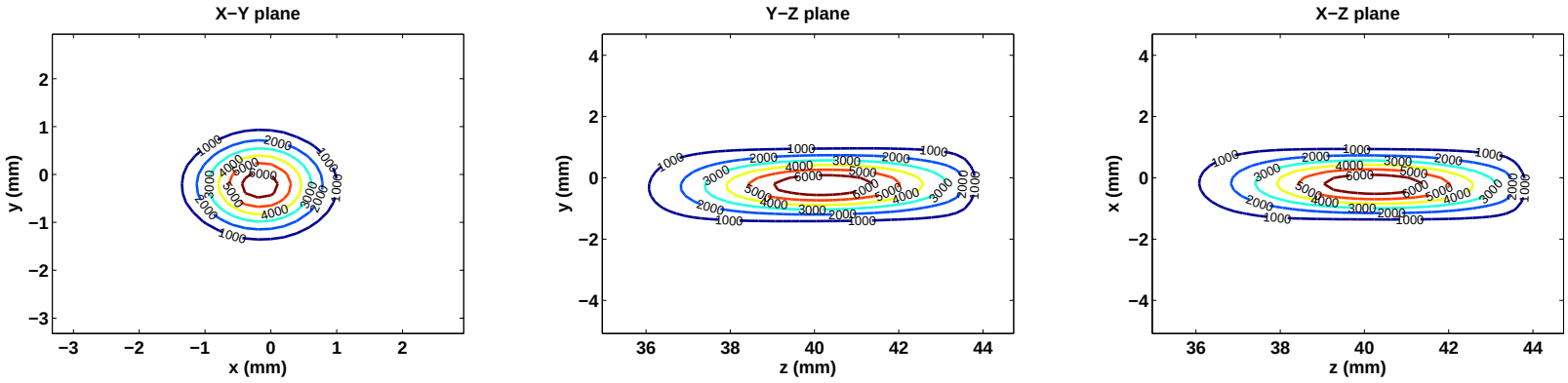

(a) (b) (c)

Figure 3.10: $670KHz$ fast marching method

3.2.10 $670KHz$ Fast Marching With Half Resolution

This case shows the robustness of FMM to resolution at even lower frequency of $670KHz$. For half resolution, spatial resolution dx= $0.3906mm$. At $670KHz$, wavelength of sound waves through water is $2.24mm$. Thus it is 5 times greater than grid spacing. Again, compared to Figure 3.7 ($1MHz$ case), the maximum amplitude is lower in this case. While it is 7000 units for $1MHz$, it is 6000 in this case. But the focus is equally sharp. Due to decrease in resolution by half, computation time decreases by 12 times. **Computation time: 1.75 *minutes***

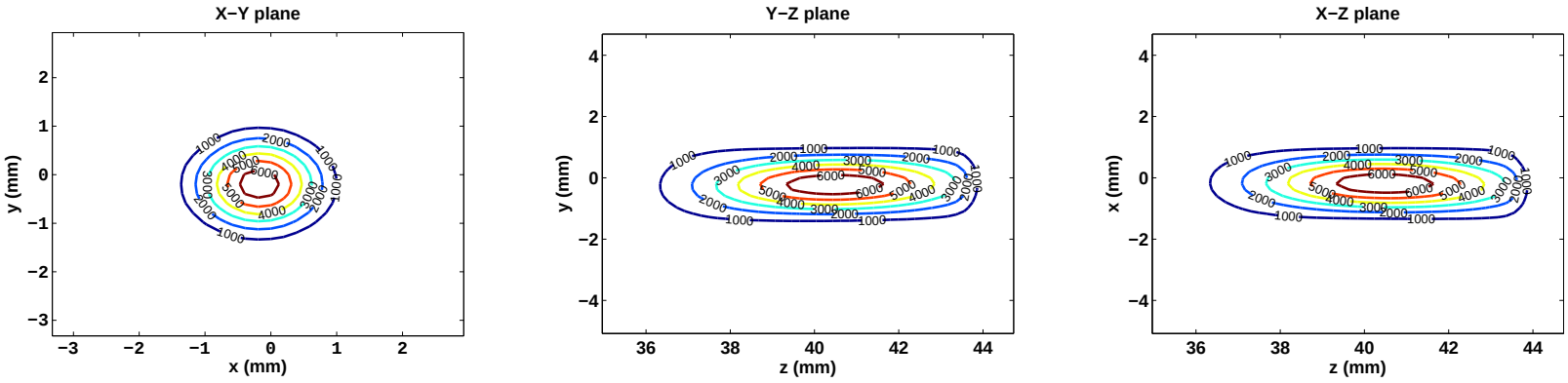

(a) (b) (c)

Figure 3.11: $670KHz$ fast marching method (half resolution)

3.2.11 $670KHz$ Fast Marching Method With Quarter Resolution

For quarter of the original resolution, dx= 0.7812. Thus there are around 2.86 grid points per wavelength of sound wave through water at this frequency. Though this resolution would have satisfied the Nyquist criterion while using k-space method, one must note the computation time in FMM case. It falls substantially from the original resolution case. Again the results in terms of sharpness and peak energy are slightly poor as compared to corresponding $1MHz$ case (Figure 3.8). **Computation time :8.2 *seconds***

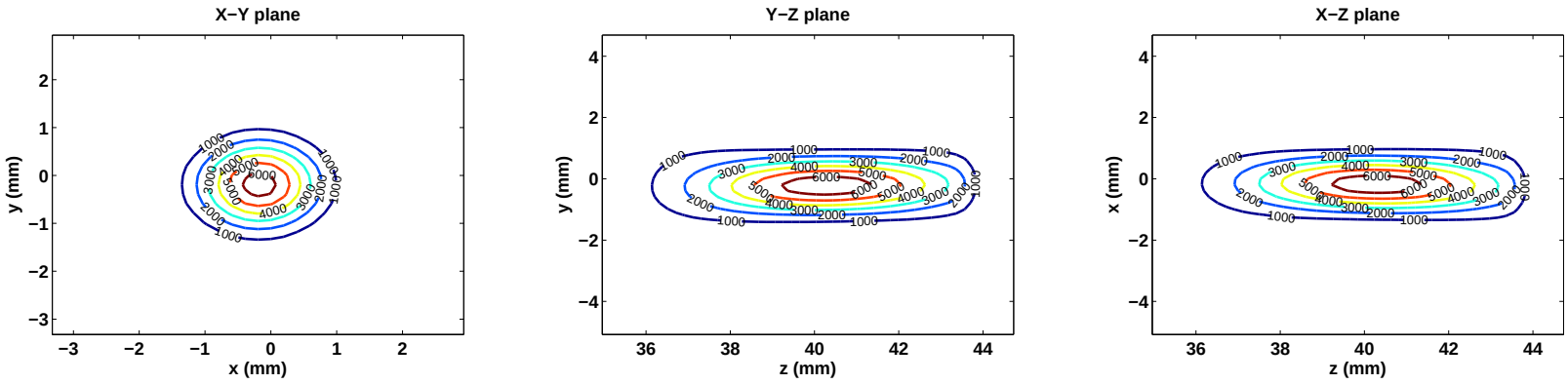

(a) (b) (c)

Figure 3.12: $670KHz$ fast marching method (quarter resolution)

3.3 *X-axis* plots

In the previous sections, results were presented to prove that FMM gives a sharp focus. In this section, comparison for amplitude of energy (squared pressure) at the focus is made for different cases. The plots shown below are the energy distribution along a line parallel to X-axis passing through the point source, hence referred to as *X-axis* plots. These results demonstrate the amount of energy concentrated at the focal point, which is an important parameter in thermotherapy. The plots also reveal the presence of side lobes, if any. They represent noise, away from the focal point, which is very undesirable parameter. Thus the results serve as an important litmus test of phase correction method under consideration. Also included are similar plots comparing the cases of transducer element averaging for $1MHz$. These provide validation towards using mean arrival time of grid points forming an element.

3.3.1 $1MHz$ Phase Correction Comparison

The first important revelation is the difference in amplitudes between the case without phase correction and others. There is also a prominent side lobe at around $1mm$ from the focal point. The difference between other cases is very marginal. FMM with half resolution has the highest acoustic energy, closely followed by FMM (original resolution) and FMM (quarter resolution). All the results are with averaging of transducer points and hence the subtle differences in the methods get more or less nullified. AS will be explained by next subsection, when averaging is done for transducer element grid points, FMM is not necessarily less accurate than k-space though theoretically that should be the case.

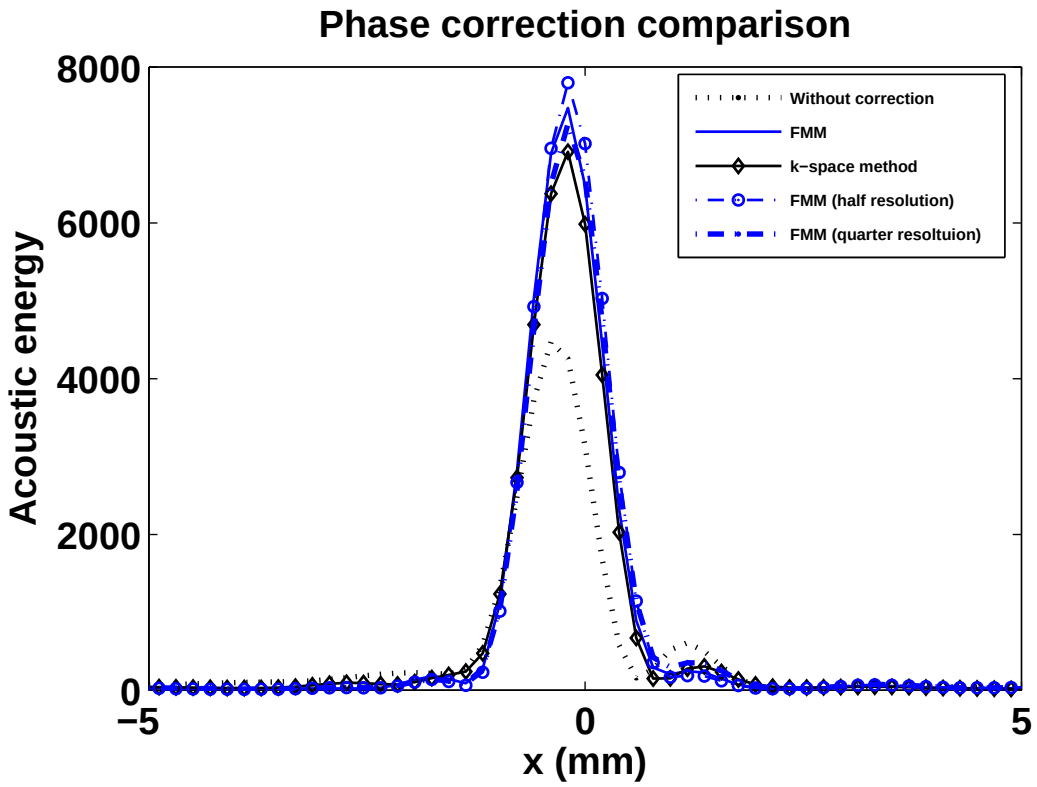

Figure 3.13: $1MHz$ Phase correction comparison

3.3.2 $1MHz$ Averaging Comparison

These results show the difference in focus with and without using average of arrival times on grid points forming each transducer element. As expected, k-space method is more accurate than FMM when arrival times on each grid point is used without averaging. The gap between k-space and FMM in this case is also slightly larger. On the other hand, averaging nullifies this difference with FMM in fact having a higher peak than k-space. Thus, when average of arrival times is used (which is realistic case as each surface of each element emits waves simultaneously) FMM is not necessarily less accurate than k-space method.

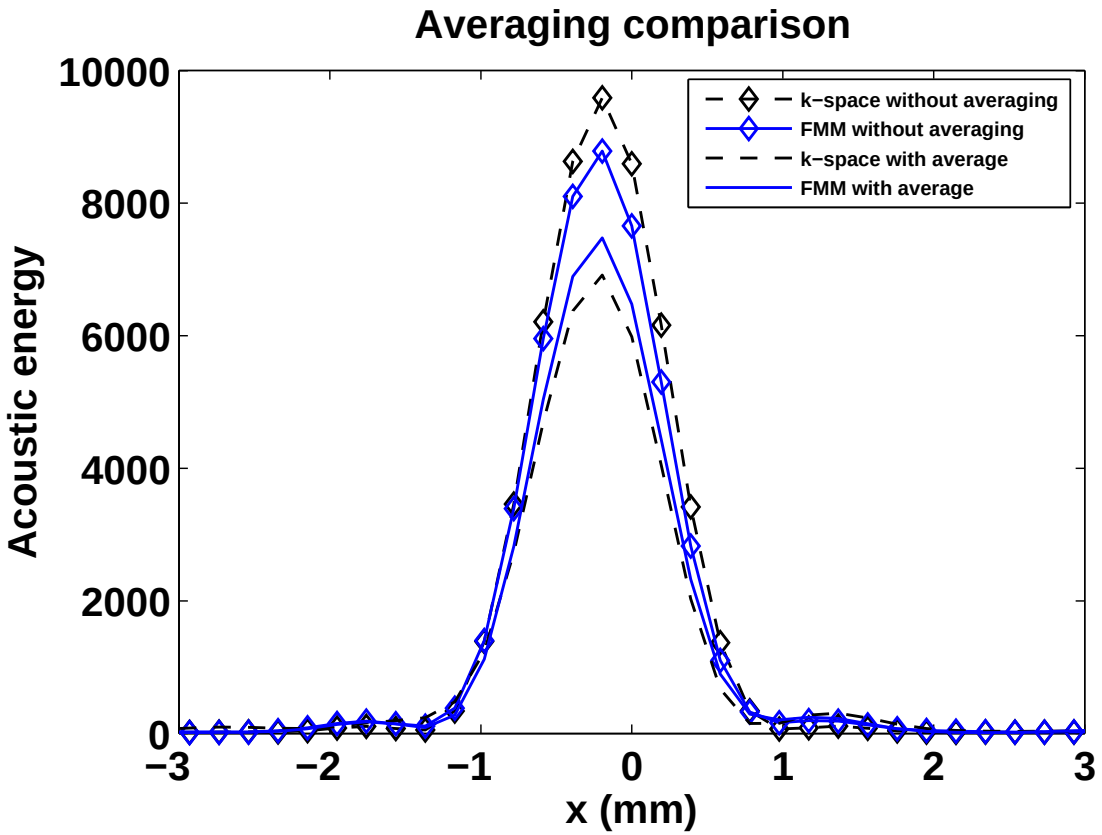

Figure 3.14: $1MHz$ Averaging comparison

3.3.3 $670KHz$ Phase Correction Comparison

Comparison of FMM for different resolutions and the case without phase correction of $670KHz$ is shown below. Without any correction, the focusing is weak and there is a prominent side lobe at around $2mm$ from the point source with energy of around 500. The focus is also shifted by around $0.4mm$. There is no significant difference between the FMM cases for different resolutions. Again, half resolution has maximum energy level closely followed by FMM for original and quarter resolutions.

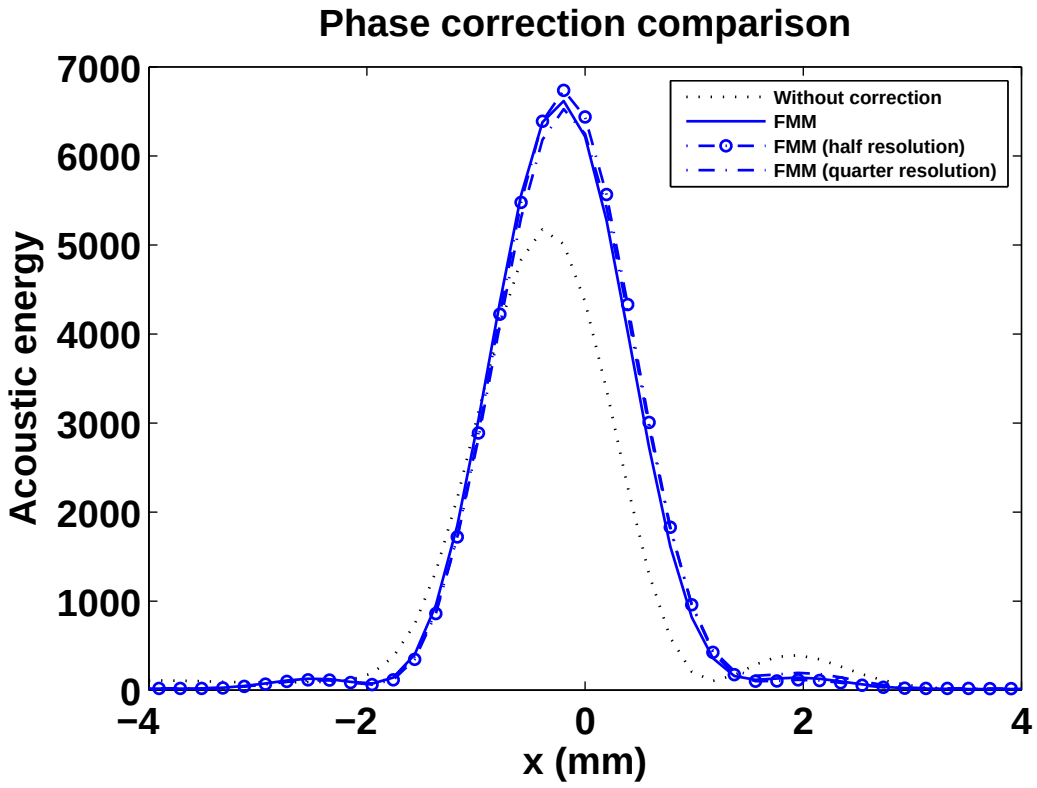

Figure 3.15: $670KHz$ Phase correction comparison

Chapter 4

Concluding Remarks

4.1 Summary of Research

High Intensity Focused Ultrasound (HIFU) is a method in which acoustic beam is focused at a point to produce maximum local heat without damage to intervening tissue. The advantage is non-invasive treatment of tumors and other abnormalities situated deep inside a tissue. Transcranial ultrasound beam focusing is an upcoming therapy in treatment of brain tumor[16][42][29][40][30][10][8], thrombolytic stroke treatment[4], drug delivery[27], Parkinson's disease[19] and other neurological disorders. Skull, however, presents a barrier to precise focusing. A time reversal method is thus used to focus ultrasound beam at a single point. The technique uses numerical excitation of focal point and phase correction of the received data at transducer location. Various methods are used for the wave propagation and phase correction. This study presented a new method: Fast Marching Method (FMM) for transcranial beam focusing. It solved Eikonal equation instead of the full wave equation. The results were compared to k-space method (a full wave equation solving method) for focus sharpness, amplitude of converged acoustic energy and com-

putation time. Two frequencies were studied, $670KHz$ and $1MHz$, taking into account past researches[37][36], high frequency approximation and attenuation through skull[18]. While the focus is equally sharp and amplitude reasonably close to the k-space value, the biggest finding was the advantage in computation time for FMM. The k-space method required around $22 - 24hours$ for any of the cases studied; the FMM had computation time in order of minutes, from $21 - 23minutes$. The FMM is also more robust to lower resolution of CT skull image and there was no significant difference to the original resolution for any of the above parameters. However, due to the use of lower resolution, the computation time decreased to around $1.75minutes$ for half resolution and about $8.2seconds$ for quarter the original resolution. Another important factor that was studied was the effect of averaging for grid points representing a transducer element. This factor has hitherto not been studied in detail. As a transducer element has finite area from which the waves will be simultaneously emitted, numerical calculations have an error when undertaken considering each element as a set of n number of grid points. The present study took up both the case, with and without averaging, and compared the results for $670KHz$ and $1MHz$. For k-space as well as FMM, the result proved that averaging is a justified and realistic assumption. The research thus opens up the possibility of a very low pre-treatment computation time and hence a quicker and convenient therapeutic process.

4.2 Future Directions

The study carried out numerical simulation and showed the viability of FMM for phase correction. This proof opens up vast number of opportunities for further research. The present study was undertaken on only a portion of skull. The reason, as has been already

stated, is the computation resource limitation for k-space method. As the results of FMM were compared with those of k-space, the latter was the limiting factor. More research can be undertaken using FMM on larger portion or complete human skull. In such cases lower resolution image can be used as the research has already proven the robustness of FMM to resolution. Also, here square transducer elements of $11.7 \times 11.7mm$ were used. Transducers with different element sizes and geometrical shapes can be used for further studies. Pernot et. al have considered variations in transkull ultrasound focusing using different array distributions like hexagonal, annular, quasi-random etc. The correction was achieved by time reversal. They noticed slight deviations in the results for different distributions[41]. Similar study can be carried out for the present method. After considerable numerical simulations have been done, ex vivo experiments can be done using either monkey or human skull. The skull speed image would be generated using computer tomography. Numerically simulating a point source at specified location relative to skull, phase computation can then be carried out in the same way as this study. Instead of the *forward simulation* of wave propagation from transducer to focal point, a real phase transducer array will be placed at the precise location where the arrival times were determined. This array would then emit phase corrected ultrasound waves. Using acoustic pressure sensor at the focal point, normalized pressure square (a form of acoustic energy) can be determined. by shifting the pressure sensor away from the focus, it can be determined whether the convergence is sharp. This study concluded with finding the sharpness of focus and acoustic energy in form of normalized square pressure. The ex vivo trials can be carried out using fresh human/ animal brain placed. Ultrasound can then be focused across a human skull on to a point inside this brain. Such an experiment will give heat generated and thermal effects on brain tissue and skull. Lesions and cavitation produced can be studied. Hence it will be possible to determine the thermal dosage, or in

other words the treatment timeand amplitude of each signal along with phase correction. After ex vivo trial, in vivo experiments can be carried out bringing the technology closer to implementation.

REFERENCES

[1] J-F Aubry, M Tanter, M Pernot, J-L Thomas, and M Fink. Experimental demonstration of noninvasive transskull adaptive focusing based on prior computed tomography scans. *The Journal of the Acoustical Society of America*, 113:84, 2003.

[2] Jakob Andreas Bærentzen. On the implementation of fast marching methods for 3d lattices. Technical report, 2001.

[3] JC Bamber and CR Hill. Ultrasonic attenuation and propagation speed in mammalian tissues as a function of temperature. *Ultrasound in medicine & biology*, 5(2):149–157, 1979.

[4] Stephan Behrens, Konstantinos Spengos, Michael Daffertshofer, Helmut Schroeck, Carl E Dempfle, and Michael Hennerici. Transcranial ultrasound-improved thrombolysis: diagnostic vs. therapeutic ultrasound. *Ultrasound in medicine & biology*, 27(12):1683–1689, 2001.

[5] AK Burov. High-intensity ultrasonic vibrations for action on animal and human malignant tumours. In *Dokl Akad Nauk SSSR*, volume 106, pages 239–41, 1956.

[6] Jason W Busse, Mohit Bhandari, Abhaya V Kulkarni, and Eldon Tunks. The effect of low-intensity pulsed ultrasound therapy on time to fracture healing: a meta-analysis. *Canadian Medical Association Journal*, 166(4):437–441, 2002.

[7] LILI Chen, GAIL ter Haar, CR Hill, M Dworkin, P Carnochan, H Young, and JPM Bensted. Effect of blood perfusion on the ablation of liver parenchyma with high-intensity focused ultrasound. *Physics in medicine and biology*, 38(11):1661, 1993.

[8] Rivka R Colen and Ferenc A Jolesz. Future potential of mri-guided focused ultrasound brain surgery. *Neuroimaging Clinics of North America*, 20(3):355–366, 2010.

[9] Martin O Culjat, David Goldenberg, Priyamvada Tewari, and Rahul S Singh. A review of tissue substitutes for ultrasound imaging. *Ultrasound in medicine & biology*, 36(6):861–873, 2010.

[10] Christakis Damianou, Kleanthis Ioannides, Venos Hadjisavvas, Nicos Mylonas, Andreas Couppis, and Demitris Iosif. In vitro and in vivo brain ablation created by high-intensity focused ultrasound and monitored by mri. *Ultrasonics, Ferroelectrics and Frequency Control, IEEE Transactions on*, 56(6):1189–1198, 2009.

[11] Edsger W Dijkstra. A note on two problems in connexion with graphs. *Numerische mathematik*, 1(1):269–271, 1959.

[12] Gerold R Ebenbichler, Celal B Erdogmus, Karl L Resch, Martin A Funovics, Franz Kainberger, Georg Barisani, Martin Aringer, Peter Nicolakis, Günther F Wiesinger, Mehrdad Baghestanian, et al. Ultrasound therapy for calcific tendinitis of the shoulder. *New England Journal of Medicine*, 340(20):1533–1538, 1999.

[13] Mathias Fink. Time-reversed acoustics. *Scientific American*, 281(5):91–97, 1999.

[14] Nicolas Forcadel, Carole Le Guyader, and Christian Gout. Generalized fast marching method: applications to image segmentation. *Numerical Algorithms*, 48(1-3):189–211, 2008.

[15] LEON A Frizzell. Threshold dosages for damage to mammalian liver by high intensity focused ultrasound. *Ultrasonics, Ferroelectrics and Frequency Control, IEEE Transactions on*, 35(5):578–581, 1988.

[16] FJ Fry. Transkull transmission of an intense focused ultrasonic beam. *Ultrasound in medicine & biology*, 3(2):179–184, 1977.

[17] FJ Fry, HW Ades, and WJ Fry. Production of reversible changes in the central nervous system by ultrasound. *Science*, 127(3289):83–84, 1958.

[18] FJ Fry and JE Barger. Acoustical properties of the human skull. *The Journal of the Acoustical Society of America*, 63:1576, 1978.

[19] FRANK J FRY. Precision high intensity focusing ultrasonic machines for surgery. *American Journal of Physical Medicine & Rehabilitation*, 37(3):152–156, 1958.

[20] William J Fry, FJ Fry, JW Barnard, RF Krumins, and JF Brennan. Ultrasonic lesions in mammalian central nervous system. *Science*, 122(3179):1091–1091, 1955.

[21] William J Fry, WH Mosberg Jr, JW Barnard, and FJ Fry. Production of focal destructive lesions in the central nervous system with ultrasound. *Journal of Neurosurgery*, 11(5):471, 1954.

[22] WJ Fry. Intense ultrasound in investigations of the central nervous system. *Advances in biological and medical physics*, 6:281, 1958.

[23] WJ Fry and R Meyers. Ultrasonic method of modifying brain structures. *Stereotactic and Functional Neurosurgery*, 22(3-5):315–327, 1962.

[24] SA Goss, LA Frizzell, and F Dunn. Ultrasonic absorption and attenuation in mammalian tissues. *Ultrasound in medicine & biology*, 5(2):181–186, 1979.

[25] M Sabry Hassouna and Aly A Farag. Multistencils fast marching methods: A highly accurate solution to the eikonal equation on cartesian domains. *Pattern Analysis and Machine Intelligence, IEEE Transactions on*, 29(9):1563–1574, 2007.

[26] CR Hill and GR Ter Haar. High intensity focused ultrasoundpotential for cancer treatment. *British Journal of Radiology*, 68(816):1296–1303, 1995.

[27] Kullervo Hynynen, Nathan McDannold, Natalia Vykhodtseva, Scott Raymond, Ralph Weissleder, Ferenc A Jolesz, and Nickolai Sheikov. Focal disruption of the blood-brain barrier due to 260-khz ultrasound bursts: a method for molecular imaging and targeted drug delivery. *Journal of neurosurgery*, 105(3):445–454, 2006.

[28] Yun Jing, F Can Meral, and Greg T Clement. Time-reversal transcranial ultrasound beam focusing using a k-space method. *Physics in medicine and biology*, 57(4):901, 2012.

[29] Ferenc A Jolesz. Mri-guided focused ultrasound surgery. *Annual review of medicine*, 60:417–430, 2009.

[30] Ferenc A Jolesz, Kullervo Hynynen, Nathan McDannold, and Clare Tempany. Mr imaging–controlled focused ultrasound ablation: a noninvasive image-guided surgery. *Magnetic resonance imaging clinics of North America*, 13(3):545–560, 2005.

[31] James E Kennedy. High-intensity focused ultrasound in the treatment of solid tumours. *Nature reviews cancer*, 5(4):321–327, 2005.

[32] JE Kennedy, GR Ter Haar, and D Cranston. High intensity focused ultrasound: surgery of the future? *British Journal of Radiology*, 76(909):590–599, 2003.

[33] Charles A Linke, Edwin L Carstensen, Leon A Frizzell, Ahmad Elbadawi, and Charlotte W Fridd. Localized tissue destruction by high-intensity focused ultrasound. *Archives of Surgery*, 107(6):887, 1973.

[34] John G Lynn, Raymund L Zwemer, Arthur J Chick, and August E Miller. A new method for the generation and use of focused ultrasound in experimental biology. *The journal of general physiology*, 26(2):179, 1942.

[35] II Marks and J Robert. *Introduction to Shannon sampling and interpolation theory*. Springer-Verlag New York, Inc., 1991.

[36] F Marquet, M Pernot, JF Aubry, G Montaldo, L Marsac, M Tanter, and M Fink. Non-invasive transcranial ultrasound therapy based on a 3d ct scan: protocol validation and in vitro results. *Physics in medicine and biology*, 54(9):2597, 2009.

[37] Nathan McDannold, Greg Clement, Peter Black, Ferenc Jolesz, and Kullervo Hynynen. Transcranial mri-guided focused ultrasound surgery of brain tumors: Initial findings in three patients. *Neurosurgery*, 66(2):323, 2010.

[38] Nathan McDannold, Mark Moss, Ron Killiany, Douglas L Rosene, Randy L King, Ferenc A Jolesz, and Kullervo Hynynen. Mri-guided focused ultrasound surgery in the brain: Tests in a primate model. *Magnetic resonance in medicine*, 49(6):1188–1191, 2003.

[39] François-Joseph Murat, L Poissonier, and A Gelet. Recurrent prostate cancer after radiotherapy: salvage treatment by high-intensity focused ultrasound. *Eur Oncol Dis*, 1:64–66, 2006.

[40] Mathieu Pernot, Jean-Francois Aubry, Mickael Tanter, Anne-Laure Boch, Fabrice Marquet, Michele Kujas, Danielle Seilhean, and Mathias Fink. In vivo transcranial brain surgery with an ultrasonic time reversal mirror. *Journal of neurosurgery*, 106(6):1061–1066, 2007.

[41] Mathieu Pernot, Jean-François Aubry, Mickaël Tanter, Jean-Louis Thomas, and Mathias Fink. High power transcranial beam steering for ultrasonic brain therapy. *Physics in medicine and biology*, 48(16):2577, 2003.

[42] Zvi Ram, Zvi R Cohen, Sagi Harnof, Sigal Tal, Meir Faibel, Dvora Nass, Stephan E Maier, Moshe Hadani, and Yael Mardor. Magnetic resonance imaging-guided, high-intensity focused ultrasound for brain tumor therapy. *Neurosurgery*, 59(5):949–956, 2006.

[43] KJW Taylor and CC Connolly. Differing hepatic lesions caused by the same dose of ultrasound. *The Journal of Pathology*, 98(4):291–293, 1969.

[44] Clare MC Tempany, Elizabeth A Stewart, Nathan McDannold, Bradley J Quade, Ferenc A Jolesz, and Kullervo Hynynen. Mr imaging–guided focused ultrasound surgery of uterine leiomyomas: A feasibility study1. *Radiology*, 226(3):897–905, 2003.

[45] GR Ter, RL Clarke, MG Vaughan, and CR Hill. Trackless surgery using focused ultrasound: Technique and case report. *Minimally Invasive Therapy & Allied Technologies*, 1(1):13–19, 1991.

[46] Bradley E Treeby and Benjamin T Cox. k-wave: Matlab toolbox for the simulation and reconstruction of photoacoustic wave fields. *Journal of biomedical optics*, 15(2):021314–021314, 2010.

[47] Bradley E Treeby and BT Cox. Modeling power law absorption and dispersion for acoustic propagation using the fractional laplacian. *The Journal of the Acoustical Society of America*, 127:2741, 2010.

[48] Bradley E Treeby, Jiri Jaros, Alistair P Rendell, and BT Cox. Modeling nonlinear ultrasound propagation in heterogeneous media with power law absorption using a

k-space pseudospectral method. *The Journal of the Acoustical Society of America*, 131:4324, 2012.

[49] Daniëlle AWM van der Windt, Geert JMG van der Heijden, Suzanne GM van den Berg, Gerben ter Riet, Andrea F de Winter, and Lex M Bouter. Ultrasound therapy for musculoskeletal disorders: a systematic review. *Pain*, 81(3):257–271, 1999.

[50] Xiaozheng Zeng, Jian Li, and Robert J McGough. A waveform diversity method for optimizing 3-d power depositions generated by ultrasound phased arrays. *Biomedical Engineering, IEEE Transactions on*, 57(1):41–47, 2010.